Phase Diagrams of Knotted and Unknotted Ring Polymers

Adam Swetnam,[1] Charles Brett,[2] and Michael P. Allen[1]

[1]*Department of Physics, University of Warwick, Coventry CV4 7AL, United Kingdom*

[2]*Department of Mathematics, University of Warwick, Coventry CV4 7AL, United Kingdom*

(Dated: March 4, 2012)

The phase diagram for a lattice ring polymer under applied force, with variable solvent quality, for different topological knot states, is determined for the first time. In addition to eliminating pseudophases where the polymer is flattened into a single layer, it is found that non-trivial knots result in additional pseudophases under tensile force conditions.

PACS numbers: 02.70.Ns,64.70.km,36.20.-r,05.10.Ln

Keywords: POLYMERS,MONTE-CARLO-SIMULATION

I. INTRODUCTION

Interest in the study of knots in both linear and ring polymers has grown dramatically in recent years. In polymeric molecules, different knot states are chemically identical but topologically distinct, so constituting a particular case of isomerism. A knot is defined by the fact that it cannot be transformed into any other knot without, in this case, breaking and remaking some of the covalent bonds. Strictly, linear polymers cannot support true knots as the ends can be pulled back through any loops to reach all other conformations. This is not the case for ring polymers, which can have genuinely different topological isomers. Knot theory is, of course, a well-developed branch of mathematics; in addition, the statistical mechanics of physical models of knotted polymers are of interest, as well as their experimental synthesis and measurements of their properties.

Knots are formally categorized according to their (minimum) crossing number when projected into two dimensions. The simplest knot is the unknot, or trivial knot, equivalent to a circle in two dimensions, with crossing number zero. There are no knots with a crossing number of one or two, one each with crossing numbers three and four (neglecting mirror images), two with crossing number five and thereafter the number increases rapidly. All of

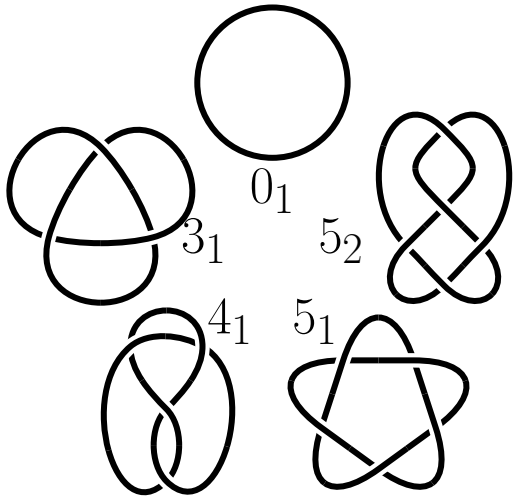

FIG. 1: Diagrams of all of the knots (neglecting chirality) with crossing number five or less: unknot (0_1), trefoil (3_1), figure-eight (4_1), cinquefoil (5_1), three-twist (5_2). Plotted using pst-knot.

these knots, with a crossing number of five or less, are prime knots (cannot be decomposed into combinations of simpler knots); they are shown in Fig. 1, with their Alexander-Briggs notation [1] in brackets.

The theoretical and computational aspects of constrained polymers, including the occurrence and effects of knots, have recently been reviewed [2]. Early simulation studies, using simple Monte Carlo algorithms and molecular dynamics, examined the knotting probability of polymer rings confined in various geometries [3, 4], while more recent work has used accelerated sampling techniques combined with histogram reweighting [5, 6].

Ring polymers with specific knot states can be synthesized [7], although this is not straightforward. It has been shown, however, that the probability of a ring containing a non-trivial knot tends to unity as the length of the polymer increases to infinity [8]. Assuming that all conformations have equal weight on formation, this implies that all sufficiently long ring polymers are highly likely to contain knots. Additionally, it has been shown that *confining* a ring polymer can affect the probability of non-trivial knots. For a ring polymer confined to a slit of decreasing width, this probability increases initially, but eventually reaches a maximum and then decreases [4]. The entropic force of the ring polymer on the walls of such a slit can also be studied. For wider slits the force decreases with increasing

complexity of the knot, while the opposite is true for narrower slits [9]. This result, and that on the probability of knots, both indicate that the number of conformations of a certain height decreases more rapidly with deviation from the entropically favoured height, as knot complexity increases. The effect of applying a force to ring polymer molecules has also been investigated [10, 11]. It is found that the force affects the probability of a non-trivial knot for finite chains, but that this probability still tends to unity in the infinite length limit. The force required in order to stretch a polymer between two walls has also been studied [12]. This involved a linear polymer with the ends grafted to parallel surfaces, containing a knot of specified topology analogous to the ring polymers.

Attempts to define knots for linear polymers date back some time [8]. One reason for this interest, is that it has been conjectured that knots are the explanation for memory effects in melts of linear polymers [13]: while, in principle, such knots can be removed, in practice this may take a long time.

It has been found that knots in linear polymers are more common in the collapsed globule phase than the random coil phase [14]. The native states of proteins, however, have been found to be noticeably deficient in knots, with only a few instances of fairly simple knots [15]. While the DNA in the nucleus of eukaryotic cells is linear, in mitochondria, bacteria and viruses, circular DNA occurs. The presence or absence of knots in DNA packaged within viral capsids is of great interest and has been studied by a combination of modelling techniques [16–19]. Topoisomerases, enzymes whose purpose is to alter the topology of DNA, are frequently studied in action on the ring-polymer form of DNA, as any knots that they introduce cannot be undone [20].

This paper reports the study of knotted and unknotted ring polymers using a simple cubic lattice model in three dimensions. For lattice polymers, there is a minimum length of ring that allows each knot to be formed on the lattice. Determining this length for different knots, and the conformations that achieve them, is a problem itself requiring numerical methods, but much progress has been made recently [21]. Using this work as a guide, it is possible to simulate, using Markov chain Monte Carlo, lattice polymers with a range of knots, down to the shortest lattice polymers known to be capable of supporting each knot. Our simulation approach involves the detailed determination of the phase diagram for a single ring polymer, using a Monte Carlo method that determines the density of states for the entire accessible range of energies and confinement in one go. Similar examples of

this approach have appeared before, notably in studies of peptide and polymer collapse, crystallization, adsorption and confinement [22–35], both on- and off-lattice.

The model, and simulation methods, will be described in section II, then the phase diagram of the isolated polymer in solution for rings of various lengths will be described in section III. The main results of the paper, concerning the effects of compressive and tensile forces on the phase diagram, will be presented in section IV. Finally, we give a summary and conclusions in section V.

II. SIMULATION METHODS

A. Lattice Polymer Model

In the most basic lattice polymer model, defined on a simple cubic lattice of spacing ℓ, each site is either occupied by a monomer bead, or is unoccupied. Successive monomers in the chain occupy adjacent sites, and chain crossings are not allowed. The effects of solvent quality and temperature are represented by an interaction energy $-\epsilon$ acting between nearest-neighbour non-bonded beads only. If a given conformation of the polymer Γ has n_Γ such contacts, the internal energy is given by $E_\Gamma = -n_\Gamma \epsilon$.

In the following, we shall be considering the effect of confinement, and of tensile forces, on the ring polymer. It will prove to be convenient to define the "force" as a thermodynamic variable conjugate to the extent of the polymer along the z-axis, i.e. its "height". Suppose that, in conformation Γ, the polymer occupies a contiguous set of h_Γ planes in the z-direction. We introduce an extra term in the energy to account for this, effectively converting it into an enthalpy H:

$$H_\Gamma = -n_\Gamma \epsilon - F \ell h_\Gamma \ ,$$

where F is the force. This definition means that positive values of F correspond to a tensile force, and negative to a compressive force. We shall choose units such that $\epsilon = 1$ and $\ell = 1$, as well as setting Boltzmann's constant k_B to unity, therefore effectively defining reduced temperatures $T^* \equiv k_\mathrm{B} T/\epsilon$ and forces $F^* \equiv F\ell/\epsilon$; the asterisk will be omitted in the following.

With these definitions, one can define a partition function and averages in the constant-

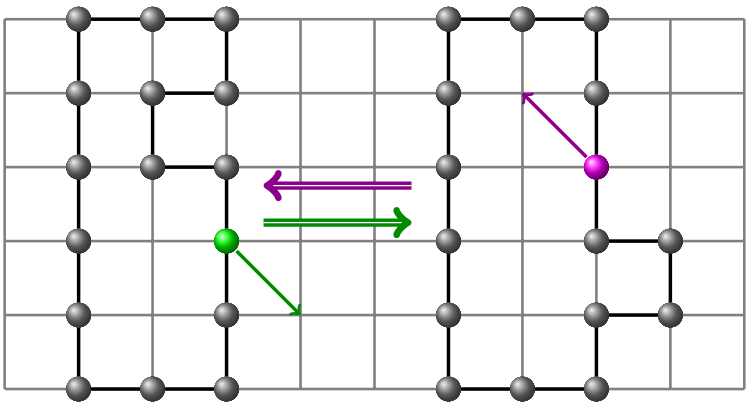

FIG. 2: (Color online) Example of a pull move, and its reverse, applied to a ring polymer.

(T, F) ensemble

$$\mathbb{Q}(T, F) = \sum_{\Gamma} \mathrm{e}^{-H_\Gamma/T} \tag{1a}$$

$$\langle A \rangle = \mathbb{Q}^{-1} \sum_{\Gamma} A_\Gamma \mathrm{e}^{-H_\Gamma/T} \tag{1b}$$

for any property A_Γ.

B. Pull Moves

As determining the knot state of a configuration of a polymer is not trivial, it might be imagined that simulation of a polymer in a certain knot state is difficult. For Markov chain Monte Carlo, however, if a move set which cannot alter the knot state is used, it is not necessary to determine the knot state of each conformation, only to have a single initial conformation which contains the knot to be simulated. The Markov chain can then be started at this conformation, and all states sampled will have the same knot. The set of pull moves [36], extended to ring polymers, is such a move set. In pull moves, a bead is moved to a site adjacent to one of its two neighbours: we refer to the direction of the chosen neighbour as 'up' the chain. Subsequent beads 'down' the chain are then moved only if this is necessary to restore the connectivity of the chain. There is a defined position for the second bead to move to, if it is moved, and subsequent beads are moved to the position previously held by the bead two places up the chain. The resulting motion resembles pulling on the chain to put 'slack' in at one point such that the slack is taken up further down the

chain. For a linear polymer, it is possible for this motion to continue until the end of the chain is reached, and a special class of end moves is required for micoscopic reversibility; this is not the case for ring polymers. An example of a pull move on a ring polymer is shown in Fig. 2. More details, and applications to the simulation of lattice polymers and peptides, may be found elsewhere [28, 36]; we have recently improved some aspects of the algorithm [29] and here we use the "unbiased pull moves" of that paper.

The proof of *reversibility* of pull moves is robust to the change to ring polymers. Although pull moves have been proved to be ergodic (complete) for linear chains, we do not know of an analogous proof for a ring with a given knot topology. Such a proof would not be trivial, but, applied to ring polymers, pull moves closely resemble moves of the BFACF algorithm, a non-length-conserving method used for lattice ring polymers. BFACF has been shown to have ergodicity classes which are the knot classes [37]. In the absence of a counter-example, we make the assumption that the pull move set is ergodic, within each knot class.

C. Density-of-States Simulations

For the simple lattice model of interest here, it is possible to obtain the partition function, for any T and F, from a single Wang-Landau Monte Carlo simulation [38], or from a set of statistically independent such simulations. The aim is to determine $\mathbb{W}(n,h)$, the number of states Γ of the system having a specified number of internal energy contacts $n_\Gamma = n$ and height $h_\Gamma = h$; we shall refer to $\mathbb{W}$ as the 'density of states'. Then, for any chosen T, F,

$$\mathbb{Q}(T,F) = \sum_n \sum_h \mathbb{W}(n,h)\, \mathrm{e}^{(n+Fh)/T} \tag{2a}$$

$$\langle A \rangle = \mathbb{Q}^{-1} \sum_n \sum_h A(n,h)\, \mathbb{W}(n,h)\, \mathrm{e}^{(n+Fh)/T} \tag{2b}$$

for any property $A_\Gamma = A(n,h)$ expressible in terms of the internal energy and the height. The specific heat capacity proves most useful in indicating phase transitions. At constant T and F, this quantity, C, can be written in terms of the fluctuations in contacts and height:

$$C(T,F) = \frac{\langle n^2 \rangle - \langle n \rangle^2}{T^2} + F^2 \left(\frac{\langle h^2 \rangle - \langle h \rangle^2}{T^2} \right) + 2F \left(\frac{\langle nh \rangle - \langle n \rangle \langle h \rangle}{T^2} \right) \equiv C^{nn} + C^{hh} + C^{nh} \ , \tag{3}$$

where it is convenient to define separate contributions from internal energy fluctuations, height fluctuations, and cross terms.

For the model of section II A, and with the force acting in the manner described, the microstates of the system are the same as those for the isolated ring polymer, so that only the internal degrees of freedom need be considered in the simulation. This would not be the case were the polymer to be bound to each surface by a specific bead, as some conformations would be excluded due to overlaps with the surfaces. The measured density of states $\mathbb{W}(n,h)$ also allows us to discuss the properties of the polymer under tension as the confining walls are pulled apart, although the geometry is not the conventional one in which beads are attracted to the walls: instead the condition is simply that at least one bead must be in contact with each of the two walls.

The density of states $\mathbb{W}(n)$ of a polymer in bulk, without any wall constraints, is trivially obtained from the full function $\mathbb{W}(n,h)$ by summing over the heights

$$\mathbb{W}(n) = \sum_h \mathbb{W}(n,h) \; .$$

Then, quantities such as the heat capacity may be determined at any desired T:

$$C(T) = \frac{\langle n^2 \rangle - \langle n \rangle^2}{T^2} \; . \tag{4}$$

Pull moves have previously been combined with Wang-Landau sampling of peptides [28]. The essential element is the replacement of the Boltzmann factors in the conventional Monte Carlo acceptance criterion by the ratio $\mathbb{W}_{\rm old}/\mathbb{W}_{\rm new}$, resulting in an asymptotic distribution of configurations with a density proportional to the inverse of $\mathbb{W}$. This results in a flat histogram $\Phi_{n,h}$ of visits to each point (n,h). In the course of the simulation, using the traditional approach, $\mathbb{W}$ is initially set equal to 1 everywhere, and the value of $\mathbb{W}(n,h)$ at each visited point (n,h) is modified according to $\mathbb{W}(n,h) \to f\mathbb{W}(n,h)$. The modification factor f is initially set to e. The simulation is broken down into stages; each stage is terminated when a "flatness condition" for the histogram $\Phi_{n,h}$ is satisfied, whereupon the modification factor f is replaced by $\sqrt{f}$.

We have recently investigated the optimization of convergence of the Wang-Landau method for lattice polymers [33]. The new version of the algorithm is based on the formula [39–41]

$$\ln f = p \sum_{n,h} \left(\phi_{n,h} - \frac{1}{N_{\rm bin}} \right)^2 = p \left(\sum_{n,h} \phi_{n,h}^2 - \frac{1}{N_{\rm bin}} \right) \; .$$

Here $\phi_{n,h}$ is the normalized visit histogram

$$\phi_{n,h} = \frac{\Phi_{n,h}}{\sum_{n,h} \Phi_{n,h}} = \frac{\Phi_{n,h}}{N_{\mathrm{MC}}}$$

where $N_{\mathrm{MC}} = \sum_{n,h} \Phi_{n,h}$ is the number of Monte Carlo moves so far. N_{bin} is the number of distinct "bins" or values of n, h accessible to the simulation, so for a flat histogram we expect the mean value $\overline{\phi_{n,h}} = 1/N_{\mathrm{bin}}$. This algorithm results in a slower variation of f with the progress of the simulation, and a much greater likelihood of convergence. The optimum prefactor p may be system-dependent; in the current work, we choose $p = 1$ as discussed in Ref. [33].

III. RING POLYMERS IN SOLUTION

First, results will be presented for the case of an isolated ring polymer molecule, representative of a dilute solution of ring polymer molecules, without any wall constraints.

The lattice model reproduces the main coil-globule transition as the temperature or solvent quality, or conversely the attractive energy parameter, of the model are varied. Additional transitions also occur as a consequence of the lattice geometry [42]. The lowest energy conformations of *linear* polymers with $N = L^3$, where L is an integer, are cubic and those with $N = L^2(L-1)$ or $N = L(L-1)^2$ are cuboid; we denote these ground-state energies (in reduced units with $\epsilon = 1$) as E_{gs}. In these cuboidal cases there are no conformations with energy $E_{\mathrm{gs}} + 1$, as displacement of a single bead results in a net decrease in the number of nonbonded contacts of at least 2. As a result, there are additional first-order pseudotransitions of lattice polymers at low temperatures, with properties which vary cyclically with the length of the polymer. It has been shown that these transitions are not true thermodynamic phase transitions [43], in the same sense as crystallization transitions of other (off-lattice, or more complicated lattice) models.

The same behaviour is seen for ring polymers on the lattice; in this case, for cuboidal ground states, as there are no end beads, at least 2 beads must be out of place in the first excited state, so that the energy gap is 3. The cycling of the properties of the transitions is demonstrated, for the unknot, by Fig. 3. It can be seen that the strength of the first transition, as measured by the height of the specific heat peak, increases as N approaches each of the critical lengths ($36 = 3^2 \times 4$, $48 = 3 \times 4^2$, $64 = 4^3$, $80 = 4^2 \times 5$, $100 = 4 \times 5^2$).

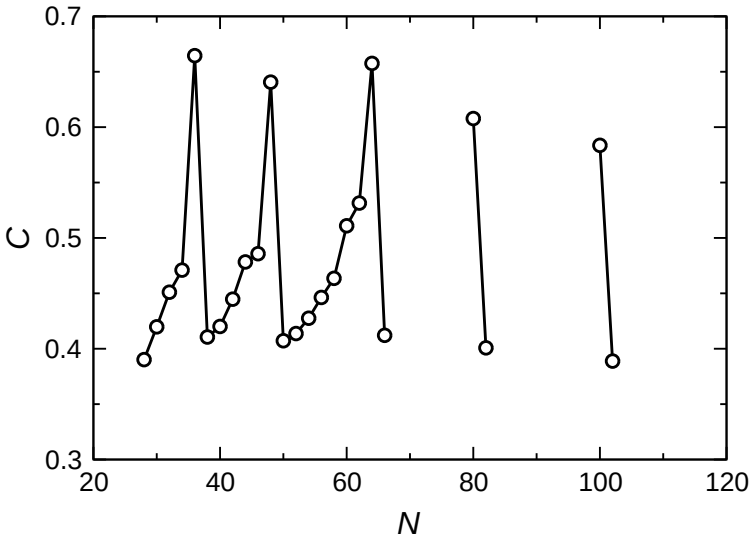

FIG. 3: Value of specific heat C at its first maximum with respect to temperature, against chain length N, for the unknot (0_1). 15 independent runs were used for each point and the standard error is less than the symbol size in all cases. The specific heat curve for the 102-bead ring polymer has an inflection point at lower temperature which could, within uncertainty, be an additional maximum followed by a minimum.

It is important for trends in the properties of transitions, as chain length increases, to be separated from any lattice effects, and that any effect of the cuboid ground states on other transitions can be determined. For this reason, ring lengths in the vicinity of these critical values were studied, for each of the knots of crossing number up to and including 5, including the unknot. In all cases, at least 15 independent runs were performed in each case in order to quantify uncertainties. The runs ranged in length from 1×10^{10} attempted moves, for the shortest ring polymers, to 8×10^{10} moves for the longest.

IV. RING POLYMERS WITH APPLIED FORCE

A. Phase Behaviour of Unknotted Rings

Fig. 4 shows the heat capacity C as a function of T and F, for the 100-bead ring polymer with no knot. Also shown is the contribution to C which arises from fluctuations in the height, as defined by eqn (3). Four ridges can be seen in the C^{hh} plot, indicating transitions in which the ensemble average of the height of the molecule changes. Two of the ridges are

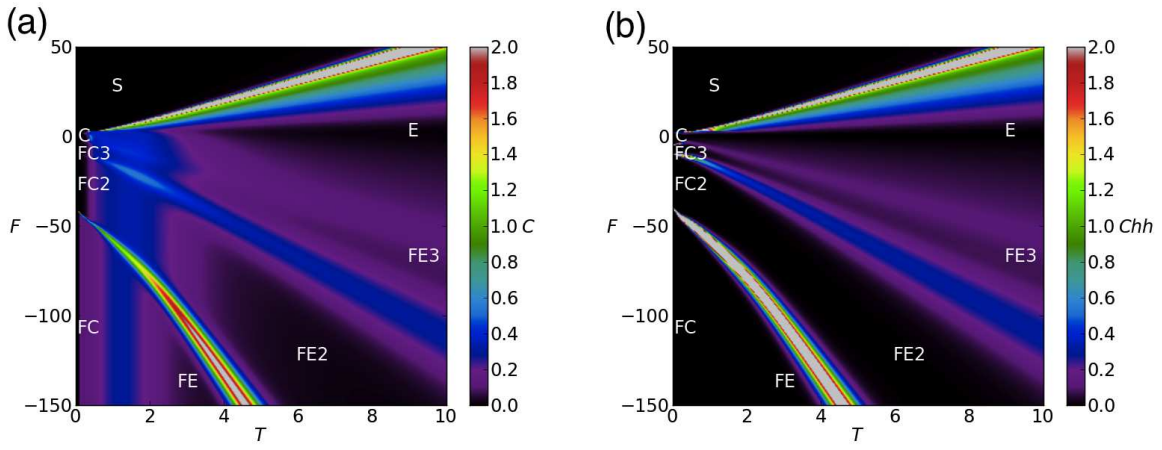

FIG. 4: (Color online) Specific heat for a 100-bead ring polymer with no knot (0_1): (a) total, C, and (b) contributions of fluctuations in height, C^{hh}. Values greater than 2 are indicated by light grey to make lower ridges perceptible. Major phases are labelled (see text).

significantly higher then the other two, implying that these transitions are much stronger. The relative height of the ridges in the specific heat will be made clear when extrapolation to the thermodynamic limit is discussed. At high T, the force at which these transitions occur is approximately linear in T. As $T \to 0$ there is a discontinuity in this trend, which relates to the collapse transitions, indicated by ridges in C at fixed T. There is no sign of the collapse transition for forces greater than the highest force ridge in C^{hh}. Between this ridge and the lowest force ridge in C^{hh}, the profile of the ridge indicating the collapse transition remains quite constant. At the lower ridge this profile changes, indicating a change in the nature of the collapse transition.

The pseudophases include the usual collapsed (C) and expanded (E) phases of the polymer near $F = 0$, at low and high temperatures respectively, as well as pseudophases where the molecule is *flattened* (F) or *stretched* (S). These include pseudophases where the polymer is flattened into a single layer, and collapsed (FC) or expanded (FE). The change in the profile of the ridge associated with collapse transitions is now explained, as part of the ridge is associated with a 3-dimensional collapse transition, and part with a 2-dimensional collapse. Additionally, there are both collapsed and expanded pseudophases of intermediate flattening of the polymer, where the polymer occupies only 2 lattice planes (FC2 and FE2) and only 3 lattice planes (FC3 and FE3). Finally, there is the stretched phase (S), where the ring is pulled tight so as to have the maximum extent along the z-axis. Representative

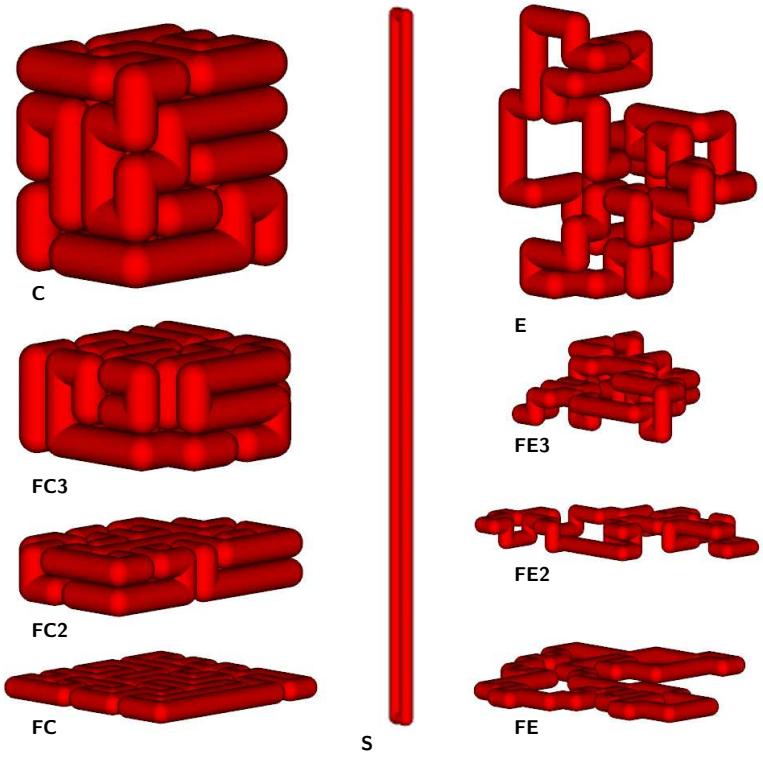

FIG. 5: (Color online) Representative conformations of each of the pseudophases of 100-bead ring polymer with no knot (0_1). The polymer is represented as a tube with a diameter equal to the lattice spacing; the z-axis points up the page.

conformations for each of these pseudophases are shown in Fig. 5.

There are, in addition, very low ridges within what has been labelled as the collapsed pseudophase. These stem from the asymmetric shape of the compact globule, caused by the underlying lattice. For $F = 0$ the energy of the system does not change depending on the orientation of the globule, so conformations of all orientations are equally likely. A small positive (negative) force, however, is sufficient to cause only those conformations with the longer (shorter) axis of the cuboid aligned along the z-axis to be sampled. As there is an entropy loss associated with this selection, the magnitude of the force required is proportional to temperature, so that there is an area of the pseudophase diagram associated with the case where all orientations are sampled. As only the possible orientations of the globule are different, not the actual conformations, these three cases have not been labelled as separate pseudophases, but subsumed into the C phase.

The pseudophase diagram for the 102-bead polymer is very similar to that of the 100-

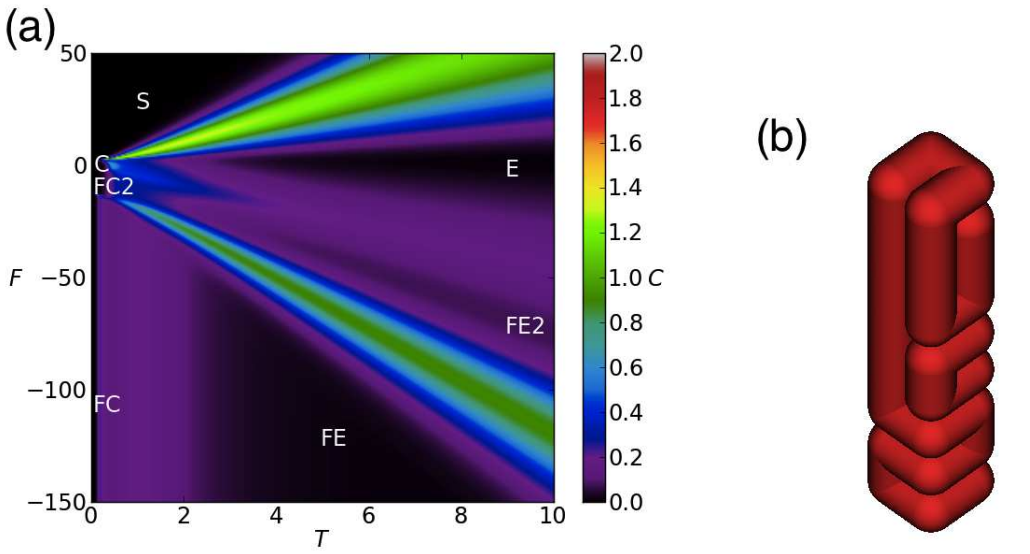

FIG. 6: (Color online) (a) Specific heat C against force and temperature for a 36-bead ring polymer with no knot (0_1). Labels indicate the location of pseudophases. (b) Representative conformation of the S2 pseudophase. The polymer is represented as a tube with a diameter equal to the lattice spacing; the z-axis points up the page.

bead polymer. The same pseudophases are seen, with only small differences in the location of the transitions between them. The minor transitions relating to the orientation of the collapsed globule remain, despite the fact that the globule is no longer cuboid. This is not surprising, as conformations with the maximum number of contacts are still asymmetric. This similarity in the phase diagram between pairs of lengths, despite the lattice effects mentioned earlier, is repeated for the other lengths studied. One case to note is the lack of any orientation transitions of the globule for the 64-bead polymer, which is easily explained by the fact that conformations with maximum contacts are those that form a cube of side 4. Other changes in the phase diagram emerge gradually with length.

The pseudophase diagram for the shortest polymer studied in detail, $N = 36$, is given in Fig. 6. It can be seen that there are no longer FC3 and FE3 pseudophases, with the system going directly directly from the C and E pseudophases to FC2 and FE2. The lack of the FC3 phases is unsurprising, as the compact globule of the 36-bead polymer has two sides of length three. An additional difference, which cannot be seen on Fig. 6, is that two ridges now separate the collapsed phase from the stretched one, with a small strip between C and S occupied by a new pseudophase S2. As can be seen in Fig. 6, conformations of this

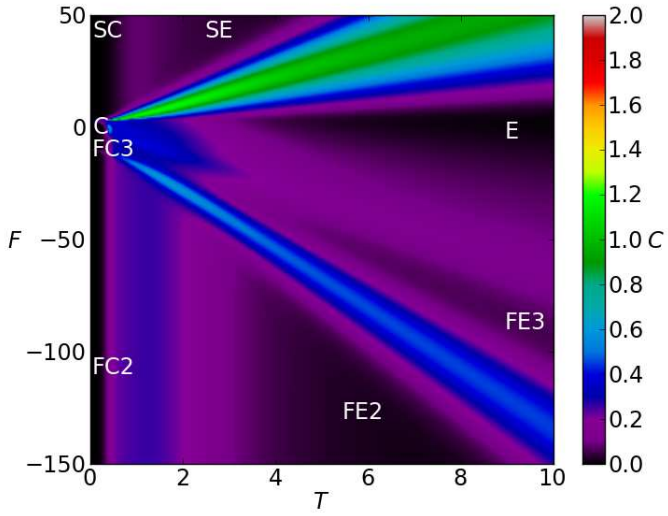

FIG. 7: (Color online) Specific heat C against force and temperature for a 100-bead ring polymer with a figure-eight knot (4_1). Labels indicate the location of pseudophases.

pseudophase have half of the maximum possible extent along the z-axis, and are compact. As a result, conformations of the S2 phase have more contacts than those of the S phase. Additionally the entropy, for the combination of contacts and height characteristic of the S2 phase, is higher than that of the maximum height. This is obvious when the disordered connection of beads in Fig. 6 is noted. The result is that the right combination of F and T favours these values of n and h.

B. Phase Behaviour of Knotted Rings

Fig. 7 shows the pseudophase diagram for the 100-bead ring polymer containing a figure-eight knot, 4_1, the unique knot with 4 crossings, while Fig. 8 shows representative conformations from each of the pseudophases. The most obvious difference with the unknot case is the absence of the flattened, single-layer, pseudophases: the regions of the phase diagram occupied by the FC and FE pseudophases are now turned over to the FC2 and FE2 pseudophases, respectively. Additionally the region previously occupied by the S phase is now divided by a ridge at constant temperature, into an SC phase, where contacts are maximized (given the constraint of maximum h), and an SE phase where expanded conformations (maximising h) are entropically favoured. The unknotted ring polymer has no such transition, as the

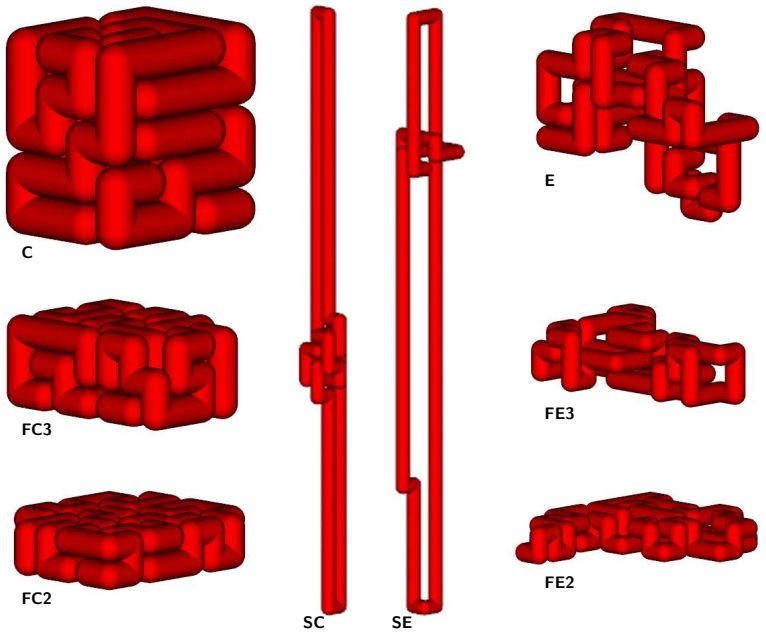

FIG. 8: (Color online) Representative conformations of each of the pseudophases for a 100-bead ring polymer with a figure-eight knot (4_1). The polymer is represented as a tube with a diameter equal to the lattice spacing; the z-axis points up the page.

number of contacts n is uniquely determined by the constraint of maximum h (specifically, when $h = N/2$, $n = h - 2$). The phase diagram is otherwise qualitatively the same as the unknot case, though the precise locations of the transitions vary.

The pseudophase diagrams for the 100-bead ring polymer with the other knots studied (those of three and five crossings) are very similar. The most notable aspect is that the strength of the SC to SE transition varies in the order $4_1 > 5_2 > 5_1 > 3_1$, i.e. the figure-eight knot transition is strongest and the trefoil weakest. For all of the lengths studied down to 48 beads this order persists. More generally, the inclusion of knots results in the same changes in the phase diagram as for $N = 100$ over this range of lengths, with the exception that three-layer phases emerge for the 48 and 50-bead polymers on the inclusion of a five-crossing knot. This is due to the extra constraints imposed on such small rings by the more complex knots; as illustrated in Fig. 9. For the unknot 0_1, the 48-bead ring polymer forms a 3×4^2 cuboid to maximize the number of contacts $n = 56$, and this ground state appears in the figure as a detached pair of points (for different orientations) at high n. However, the 5_2 knot eliminates conformations with this many contacts. As a consequence, conformations

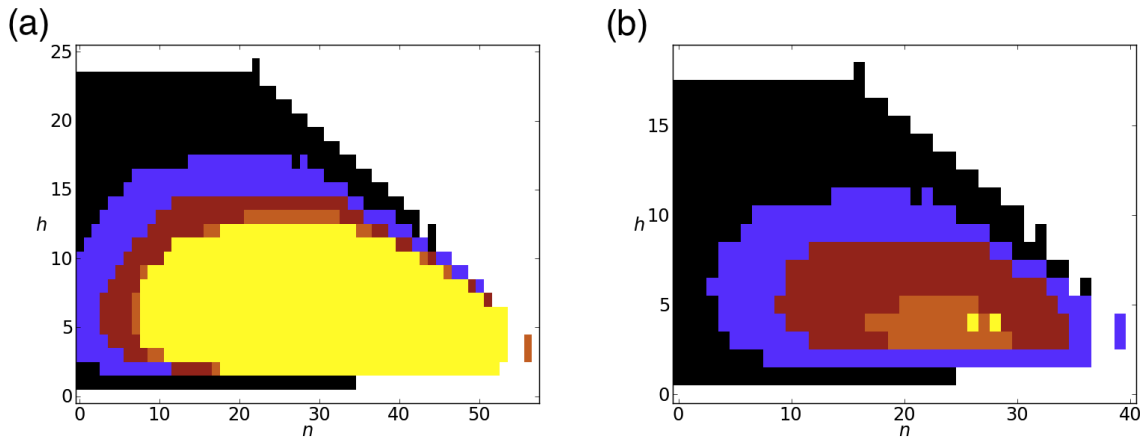

FIG. 9: (Color online) Available combinations (n, h) for ring polymers with (a) $N = 48$ and (b) $N = 36$ showing the increasing restrictions imposed by more complex knots: 0_1 (black, largest region); 3_1 (blue); 4_1 (red); 5_1 (orange); 5_2 (yellow, smallest region).

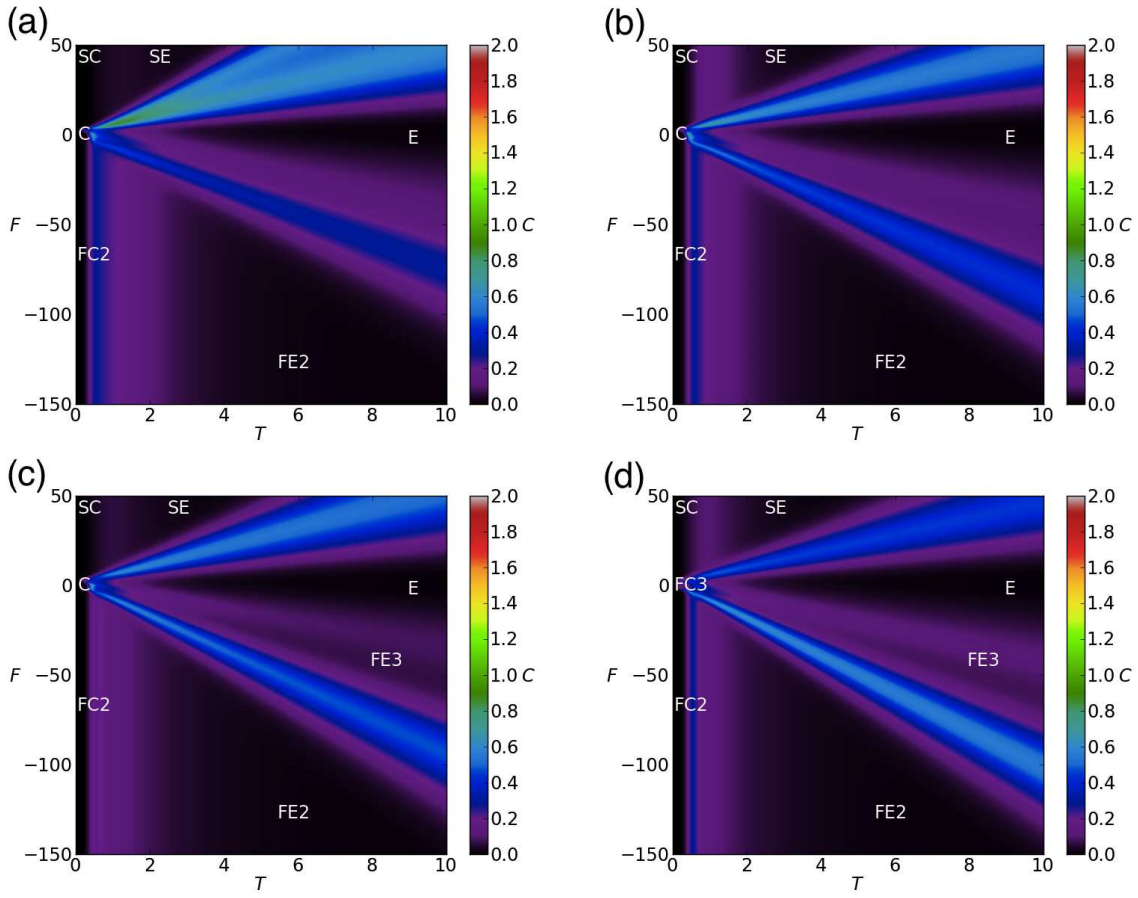

FIG. 10: (Color online) Specific heat C vs T, F for $N = 48$ ring polymers with knots: (a) 3_1; (b) 4_1; (c) 5_1; (d) 5_2.

occupying at least four lattice planes along each axis can have as many contacts as those occupying only three along one axis, and are more numerous. Thus conformations with $h = 4$ dominate at sufficiently low $|F|$, due to entropy, and only at sufficiently negative F do conformations with the same number of contacts but $h = 3$ prevail. The effect of knots on the phase diagram does not seem to be subject to lattice artefacts. The sequence of heat capacity maps for $N = 48$ is shown in Fig. 10.

Unsurprisingly the more complex knots have a more substantial effect on the shortest ring polymers studied. For the 36-bead polymer, the trefoil knot 3_1 has the same effect as for $N = 100$: the single layer pseudophases (FC and FE) are eliminated, and the S phase is divided into SC and SE pseudophases. The figure-eight knot 4_1 has the additional effect that FC2 and FE2 are replaced by FC3 and FE3 respectively, with two-layer conformations no longer available, and the completely collapsed ground-state globule is eliminated as a separate pseudophase, so that there is a transition directly from SC to FC3. With the cinqefoil knot 5_1, the number of available combinations of (n, h) is dramatically reduced, and the three-twist 5_2 is so restrictive that the simulations find only two bins with a difference of two contacts between them, and density of states equal within statistical uncertainty. This is not surprising as the 36-bead polymer is the shortest which can contain a three-twist knot [21]. Consequently, there is only a very weak collapse transition, below which conformations with the maximum contacts dominate.

C. Transition Distributions

The nature of the transitions can be investigated by plotting the joint probability distribution $P(n, h)$ for internal contacts n and height h, at values of T and F near the peaks in C, which indicate the transitions. Fig. 11 shows this for the 100-bead ring polymer with no knot, well away from transitions, in the expanded E phase at $T = 6$, $F = 0$. This serves to illustrate the general landscape. The grey region delimits the possible combinations of n and h; the ground state can be seen as a detached pair of points $(n, h) = (135, 4), (135, 5)$ corresponding to the different orientations of a $5 \times 5 \times 4$ cuboid. The E pseudophase is characterized by a relatively broad distribution of values of n and h, as would be expected. Superimposed on this same plot, for convenience and economy of space, are the extremely sharply double-peaked distributions seen for two pseudophase changes at low temperature,

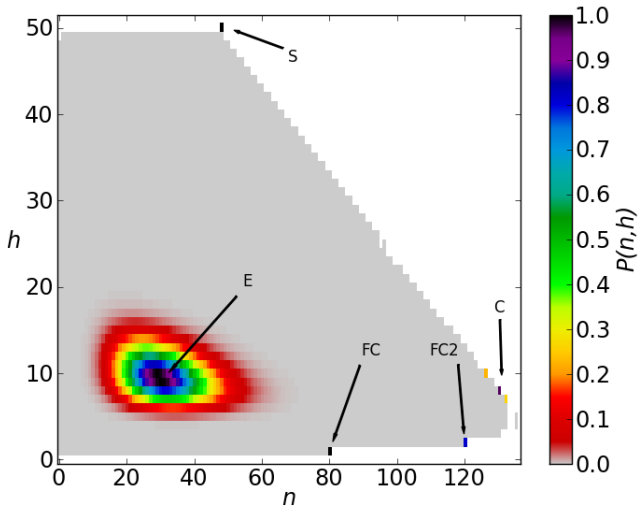

FIG. 11: (Color online) Probability distribution $P(n, h)$ (normalized by its maximum value) for contacts n and height h, for the 100-bead polymer with no knot (0_1) at $(T, F) = (6, 0)$. Superimposed on this are the very sharp distributions near the C-S transition at $(T, F) = (0.05, 2.0007)$, and near the FC2-FC transition at $(T, F) = (0.05, -41.36)$ (see text). White areas represent impossible combinations of n and h.

$T = 0.05$: the collapsed-stretched (C-S) transition and the layering transition between FC2 and FC pseudophases. The S phase at this temperature is essentially a single point, $(n, h) = (48, 50)$. At a force value $F \gtrsim 2$, an approximately equal probability weight appears in a very small cluster of points near the maximum possible n and rather small h: the C phase. The trade-off between n and h can be seen, as the jagged edge of the allowed region of combinations of n and h between these two peaks. The gradient of this edge is $\mathrm{d}h/\mathrm{d}n \approx -0.5$, so it corresponds roughly to a line of constant enthalpy at $F \approx 2$, confirming that the transition is driven by competing energy terms. The FC2-FC case typifies the layering transitions in the compact phases. There are two sharp peaks, $(n, h) = (80, 1), (120, 2)$, both at vertices of the allowed region, along the lower edge. At low temperature, the transition between them occurs at $F \lesssim -40$. For $F = -40$, these two phases have equal enthalpies $H = -n - Fh = -40$, indicating that this pseudo-first-order transition is also driven primarily by competing energy terms, rather than entropy, at this low temperature.

The layering transitions at higher temperatures, when the polymer is expanded, are quite different. Three examples are shown in Fig. 12, showing how the ring polymer is compressed

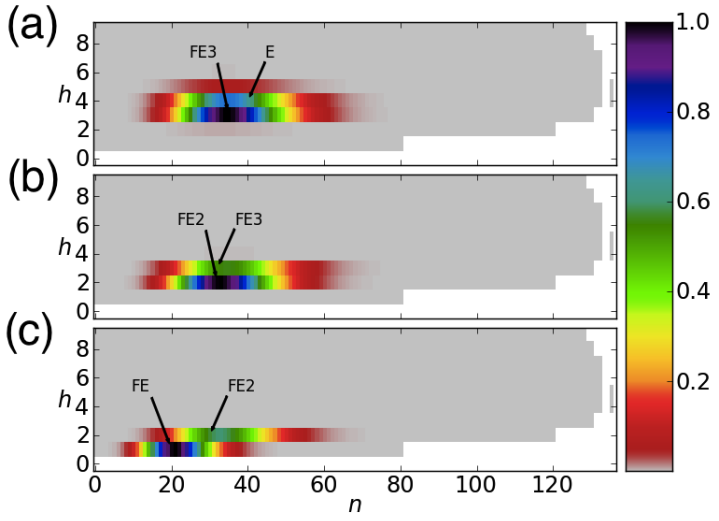

FIG. 12: (Color online) Probability distribution $P(n, h)$ for contacts n and height h, for the 100-bead polymer with no knot (0_1) at $T = 6$, showing the low-h region in detail. (a) $F = -34.3$, near the E-FE3 transition; (b) $F = -69$, near the FE3-FE2 transition; (c) $F = -192.2$, near the FE2-FE transition.

from the E phase down to a single layer, F. As the force F becomes more negative, the broad $P(n, h)$ peak of the E phase, shown in Fig. 11, shifts to lower h. The E-FE3 and FE3-FE2 transitions are rather broad, as shown in Fig. 4. Close to each of these transitions, the probability distributions $P(n, h)$ show a single peak which is broad along the n axis, but narrow with respect to h. This peak is not at the edge of the allowed (n, h) region, indicating a competition between entropy and energy in this parameter range. These transitions seem to involve only the movement of the maximum of this peak from one integer height to the next; without the lattice there would be a continuum of heights, so it seems likely that these transitions are simply an effect of the lattice.

For FE2-FE, also shown in Fig. 12, the situation is different. In this case the probability mass resides completely in the $h \leq 2$ region. However, once more, the probability mass is detached from the extremes of the allowed (n, h) range, suggesting again a competition between entropy and energy. The distribution across n is broader for $h = 2$ than for $h = 1$, with the result that there are apparently two distinct maxima. These maxima are separated, however, only by the discretization in height, caused by the lattice on which the polymer resides. An off-lattice model would have a continuum of heights, so the discontinuous nature

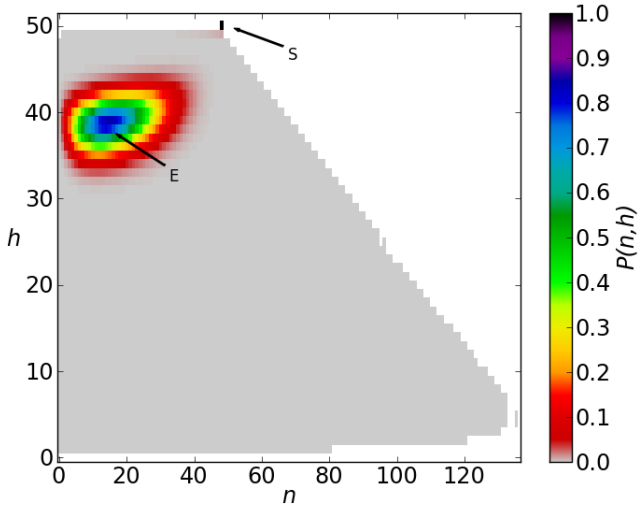

FIG. 13: (Color online) Probability distribution $P(n, h)$ for contacts n and height h, for the 100-bead polymer with no knot (0_1), at $(T, F) = (6, 28.3)$, near the E-S transition.

of this transition might only be a lattice effect; however a transition of some sort to the flattened globule must be expected, even in the absence of the lattice.

The transition between the E and S phases, for which the probability distribution is shown in Fig. 13, is clearly not a lattice effect. In this case there is a broad peak, corresponding to those conformations with a relatively large h, which are representative of the expanded pseudophase, and a sharp peak representative of maximum height conformations, for which the number of contacts n is uniquely determined. Again this transition relates to the fact that the combinations of n and h of the expanded pseudophase have higher entropy, but those of the stretched phase have lower energy at sufficiently high force. In this case there are valid (n, h) combinations in the region between these two peaks, but the entropy of these is low, making them improbable, even in this parameter range where regions either side are more probable.

The remaining transitions for the polymer with no knot are the collapse transitions, in two and three dimensions, which have been well studied. We conclude this section by examining the SC-SE transition, which occurs in the knotted rings. Fig. 14 shows $P(n, h)$ near this transition for the 100-bead polymer with a figure-eight knot (4_1). The peak actually has two maxima, but this is likely only an effect of the lattice. The figure also shows how the range of heights h is reduced, in the knotted case. There are no conformations of height 1, and

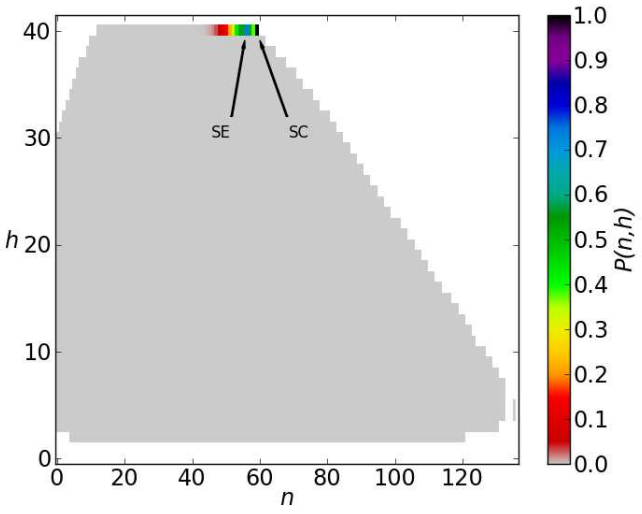

FIG. 14: (Color online) Probability distribution $P(n, h)$ for contacts n and height h, for the 100-bead polymer with the figure-eight knot (4_1), at $(T, F) = (1.04, 50)$, near the SC-SE transition.

additionally there are no conformations with $(h, n) = (2, 0)$, as the knot enforces crossings, which correspond to contacts in a two-layer conformation. Finally, as the maximum height is approached, the minimum number of contacts increases. This presumably relates to the knot being pulled tight as the polymer is stretched, creating contacts.

D. System-Size Dependence

While the range of N explored in this study is not sufficient for a quantitative finite-size scaling analysis, particularly since cyclic effects of the lattice must be eliminated from any extrapolation, it is still informative to examine the N-dependence of the specific heat measurements. Fig. 15 shows the specific heat curve, with respect to force, at low temperature. The peaks for $F < -10$ indicate the transition between the FC and FC2 pseudophases. The values of F at the transition are approximately proportional to N. The peak heights do not vary monotonically with N, even though the lengths used are from the same point in the lattice effects cycle. Much smaller peaks, corresponding to the FC2-FC3 and FC3-C transitions, can be seen for $-10 < F < 0$. Even smaller peaks occur at $F \gtrsim 0$ relating to the rotation of the globule, as discussed earlier; these are not shown in the figure. Finally, for tensile forces, peaks relating to the transitions between the C, S2 and S phases are apparent.

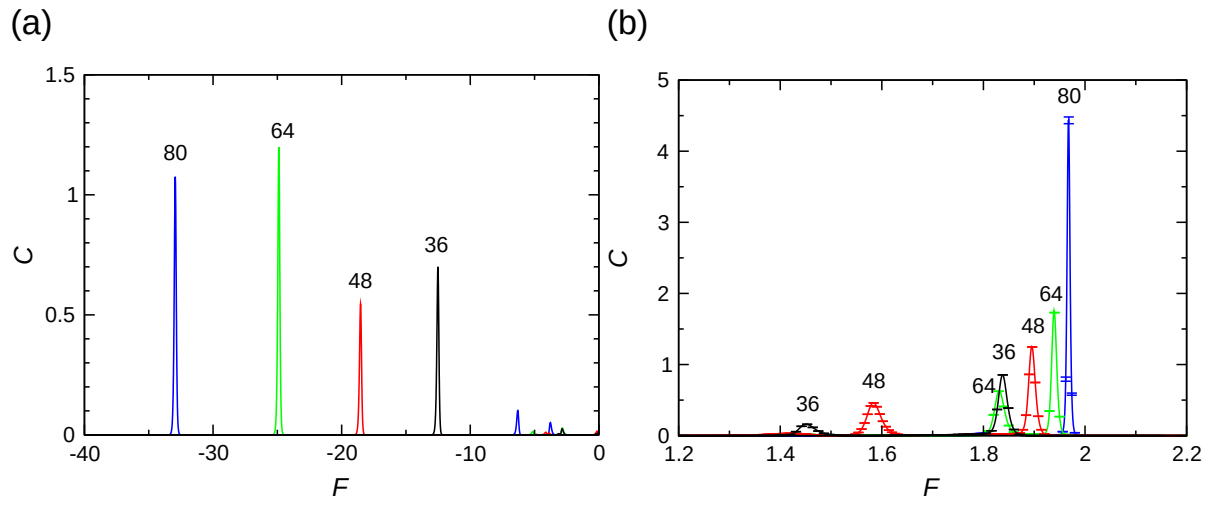

FIG. 15: (Color online) Specific heat C vs force F, at $T = 0.05$, for a ring polymer with no knot (0_1), of length (principal peaks labelled) $N = 36$ (black), 48 (red), 64 (green) and 80 (blue). (a) Compressive force region; (b) tensile force region around the C-S2-S phase transitions.

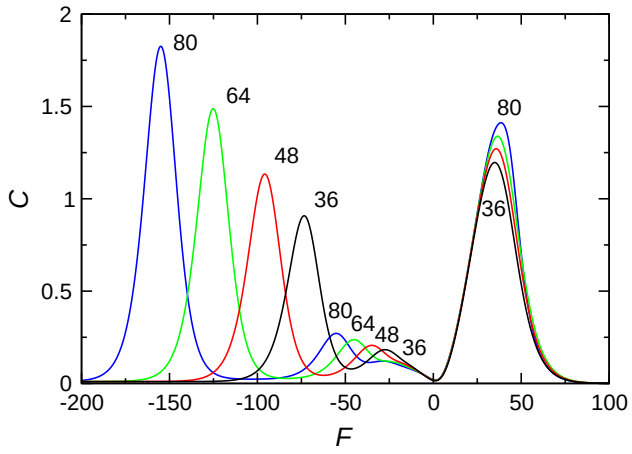

FIG. 16: (Color online) Specific heat C vs force F, at $T = 6$, for a ring polymer with no knot (0_1), of length (principal peaks labelled) $N = 36$ (black), 48 (red), 64 (green) and 80 (blue).

Fig. 15 shows this region in detail. It can be seen that for all but the 80-bead polymer there are two transitions, one from the C to the S2 pseudophase then, at greater force, another from the S2 pseudophase to S. These transitions converge together as N increases until there is only a single transition, from C directly to S, for the 80-bead polymer. The height of the peaks increases with length, indicating that this pseudotransition corresponds to a true phase transition in the thermodynamic limit, and the position of the peak seems to be converging to a value $F \approx 2$.

Fig. 16 shows the specific heat curve, with respect to force, at a high temperature where the expanded phases are most stable. The peaks at the most compressive forces, $F < -70$, indicate the transition between the FE and FE2 pseudophases. As for the corresponding results at low temperature, the transition shifts to increasingly negative forces with increasing length, but this time the specific heat peak also increases in height monotonically with N. The smaller peaks in the range $-70 < F < 0$ indicate the transitions between the FE2, FE3 and E phases, which are thought to be only an effect of the lattice. Finally, the peaks for $F > 0$ mark the E-S transition. This peak only sharpens and shifts slightly as N increases, again indicating a true phase transition in the thermodynamic limit.

V. CONCLUSIONS

In this paper, we have presented an overview of the phase behaviour, determined by Wang-Landau simulations, of ring polymer molecules whose monomers have a nearest-neighbour attraction, and which are subjected to compressive and tensile forces. The effect of knots of up to five crossings on the phase stability, and the positions of phase transitions, was investigated. Ring polymers of up to $N = 102$ beads were studied, using pull moves, and an algorithmic trick (described in the appendix) employed to ensure effective sampling of single layer conformations for the longer polymers. The phase diagram was determined by plotting the specific heat C against temperature T and force F, with additional insight obtained from the separate contributions of fluctuations in height h and internal contacts n, and from inspection of the joint probability distributions $P(n, h)$ near the transitions.

For the unknotted ring (0_1), the normal expanded and collapsed phases were observed at sufficiently low F. Additionally, a single stretched pseudophase, thought to correspond to a true phase in the thermodynamic limit, was found for large positive (tensile) forces F. It is suggested that the transitions to this phase, from the collapsed and expanded phases, are likely to be first-order at large N, with that from the expanded phase being related to the competition between entropy and energy, and that from the collapsed phase being energetically driven. On compression, pseudophases where both the compact globule and the expanded coil were squeezed into ever fewer lattice planes were discovered. These layering transitions seemed to be continuous for the expanded coil, and it is thought that there are only multiple transitions in this case due to the underlying lattice. For the globule, these

transitions are not thought to be lattice effects, and are found to be energetically driven, and first-order in character. It is unclear whether any of these pseudophases correspond to true thermodynamic phases, as the transitions to them move to increasingly negative force as N increases. For shorter polymers there is an intermediate, partially-stretched, pseudophase, but this is eliminated before N reaches 80.

The introduction of a knot into the polymer results in some general alterations to the pseudophase diagram. First, the pseudophases where the polymer is flattened into a single layer are eliminated, an inevitable result of the excluded volume and the crossing(s) associated with projecting the knot into two dimensions. Secondly, an additional transition divides the stretched phase into collapsed and expanded pseudophases. The reason for this is that the knot gives rise to a non-unique number of internal contacts n, for a ring maintained at the maximum possible h, whereas n is uniquely determined for the unknot. In addition to these general effects, as knots of increasing crossing number are included, in the shorter polymers, the pseudophase behaviour is increasingly hindered, as the knot restricts the possible values of n and h.

This work is the foundation of a more detailed study of the effects of confinement on knots and the forces exerted by knotted rings within narrow slits. For this system, it is straightforward to relate $\mathbb{W}(n,h)$ to the density of states $\mathbb{W}_{\text{slit}}(n,H)$ of a polymer confined within two parallel walls a distance H apart, by counting the number of states that satisfy the condition $h_\Gamma \leq H$:

$$\mathbb{W}_{\text{slit}}(n,H) = \sum_{h=1}^{H} (H-h+1)\,\mathbb{W}(n,h)\,.$$

Corresponding ensemble averages are obtained through equations similar to (2). Consequently, a very wide range of results, at specified T and for any choice of slit width H, can be obtained from a single simulation. It is also possible to convert these results into the constant-T,F ensemble, but in this case, states of tension are unphysical (the partition function will diverge for $F \geq 0$), and interest lies only in values $F < 0$. In addition, the determination of the phase diagrams in this work is a pre-requisite for further investigation of knot localization in such polymer models. These extensions of the current study will be the subject of future publications.

Acknowledgments

Computer facilities were provided by the Centre for Scientific Computing at the University of Warwick.

Appendix: Accessing Single Layer Conformations

In this appendix we detail the special method necessary to sample configurations of the longer unknotted ring polymers, with $N \gtrsim 60$, and small values of h. Initial simulations for these longer ring polymers with no knot found no conformations with $h = 1$, i.e. occupying only a single lattice plane, although for smaller N they were readily observed. This problem arose because the fraction of *attempted* moves which would take the system from the $h = 2$ configurations to those with $h = 1$ became vanishingly small. (Pull moves for ring polymers change h by at most ± 1). This is illustrated by a set of simulations in which the system was restricted to sample from the density of states $\mathbb{W}(n, h = 2)$ determined by Wang-Landau sampling (flat sampling across the number of nearest neighbour contacts, but height restricted to $h = 2$). The results of attempted moves could be split into four categories: those that resulted in invalid conformations, those that did not change the height, those that increased it and those that decreased the height to 1. Fig. 17 shows how the fraction of attempted moves that fall into this last category decreases exponentially with N. It is this trend which is responsible for the poor sampling of single layer conformations.

The reason for this is straightforward to understand on combinatorial grounds. Pull moves move a *maximum* of 2 beads to previously unoccupied positions. Amongst the $h = 2$ conformations, only those with exactly 2 beads in one of the layers can be transformed into single layer conformations, and the ring geometry requires that these two beads will be adjacent. It is reasonable to assume that the probability of such an excursion into the second layer will approach a constant value per unit length of polymer, say α. Consequently, the probability of observing *only one* such excursion is proportional to a product of the form $\alpha \times (1 - \alpha)^n$, where $n \sim N$, and hence this product should decrease exponentially with N, as confirmed by Fig. 17.

One solution to this problem would be to allow a wider range of moves connecting configurations with $h = 2$ and $h = 1$. The additional moves would have to move many beads

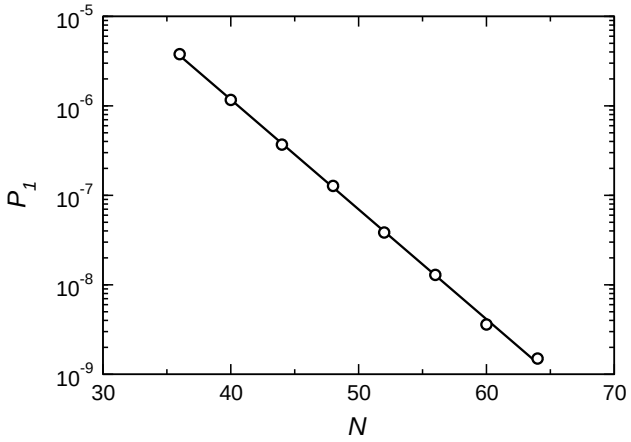

FIG. 17: Fraction of proposed moves P_1 to valid conformations of height $h = 1$, from conformations of height $h = 2$ sampled uniformly with respect to internal contacts. 10^{10} moves were attempted for each point.

cooperatively, and it would be essential to ensure detailed balance.

A simpler solution, adopted here, is to change the way Wang-Landau sampling is applied. The conformations with $h \leq 2$ and each value of n are further subdivided according to the number of beads m in one layer; as the simulation progresses, sampling of $\mathbb{W}(n, h, m)$ will be increasingly uniform across the values of m. As a result those $h = 2$ conformations having $m = 2$, with viable pull moves to single layer conformations $h = 1$, $m = 0$, are sampled preferentially. The density of states $\mathbb{W}(n, h = 2)$ can then be determined simply as the sum $\sum_m \mathbb{W}(n, h = 2, m)$. It is sufficient to define $m = \min(m_1, m_2)$ where m_i is the number of beads in layer i. It is not necessary to subdivide other values of h according to the number of beads in the various layers. This method was used for polymers of $N \geq 58$ beads.

[1] J. W. Alexander and G. B. Briggs, Ann. Math. **28**, 562 (1926).

[2] C. Micheletti, D. Marenduzzo, and E. Orlandini, Physics Reports **504**, 1 (2011), ISSN 0370-1573.

[3] J. P. J. Michels and F. W. Wiegel, Proc. Roy. Soc. Lond. A **403**, 269 (1986), ISSN 1364-5021.

[4] M. C. Tesi, E. J. J. van Rensburg, E. Orlandini, and S. G. Whittington, J. Phys. A Math. Gen. **27**, 347 (1994).

[5] C. Micheletti, D. Marenduzzo, E. Orlandini, and D. Summers, J. Chem. Phys. **124** (2006),

ISSN 0021-9606.

[6] C. Micheletti, D. Marenduzzo, E. Orlandini, and D. W. Sumners, Biophys. J. **95**, 3591 (2008), ISSN 0006-3495.

[7] C. O. Dietrich-Buchecker and J.-P. Sauvage, Angew. Chem. **28**, 189 (1989).

[8] D. W. Sumners and S. G. Whittington, J. Phys. A Math. Gen. **21**, 1689 (1988).

[9] R. Matthews, A. A. Louis, and J. M. Yeomans, Molec. Phys. **109**, 1289 (2011).

[10] E. J. J. van Rensburg, E. Orlandini, M. C. Tesi, and S. G. Whittington, J. Phys. A Math. Gen. **41**, 025003/1 (2008).

[11] M. Atapour, C. E. Soteros, and S. G. Whittington, J. Phys. A Math. Gen. **42**, 322002/1 (2009).

[12] O. Farago, Y. Kantor, and M. Kardar, Europhys. Lett. **60**, 53 (2002).

[13] P.-G. de Gennes, Macromolecules **17**, 703 (1984).

[14] M. L. Mansfield, J. Chem. Phys. **127**, 244902/1 (2007).

[15] W. R. Taylor, Nature **406**, 916 (2000).

[16] J. Arsuaga, R. Tan, M. Vazquez, D. Sumners, and S. Harvey, Biophys. Chem. **101**, 475 (2002), ISSN 0301-4622.

[17] J. Arsuaga, M. Vazquez, P. McGuirk, S. Trigueros, D. Sumners, and J. Roca, Proc. Nat. Acad. Sci. **102**, 9165 (2005), ISSN 0027-8424.

[18] J. Arsuaga and Y. Diao, Comput. Math. Meth. Med. **9**, 303 (2008), ISSN 1748-670X.

[19] D. Marenduzzo, E. Orlandini, A. Stasiak, D. W. Sumners, L. Tubiana, and C. Micheletti, Proc. Nat. Acad. Sci. **106**, 22269 (2009), ISSN 0027-8424.

[20] S. A. Wasserman and N. R. Cozzarelli, Science **232**, 951 (1986).

[21] R. Scharein, K. Ishihara, J. Arsuaga, Y. Diao, K. Shimokawa, and M. Vazquez, J. Phys. A Math. Gen. **42**, 475006/1 (2009).

[22] M. Bachmann and W. Janke, J. Chem. Phys. **120**, 6779 (2004).

[23] M. Bachmann and W. Janke, Phys. Rev. Lett. **95**, 058102/1 (2005).

[24] M. Bachmann and W. Janke, Phys. Rev. E **73**, 020901/1 (2006).

[25] M. Bachmann and W. Janke, Phys. Rev. E **73**, 041802/1 (2006).

[26] F. Rampf, K. Binder, and W. Paul, J. Polym. Sci. B **44**, 2542 (2006).

[27] J. Luettmer-Strathmann, F. Rampf, W. Paul, and K. Binder, J. Chem. Phys. **128**, 064903/1 (2008).

[28] T. Wüst and D. P. Landau, Comput. Phys. Commun. **179**, 124 (2008).

[29] A. D. Swetnam and M. P. Allen, Phys. Chem. Chem. Phys. **11**, 2046 (2009).

[30] M. P. Taylor, W. Paul, and K. Binder, Phys. Rev. E **79**, 050801/1 (2009).

[31] M. P. Taylor, W. Paul, and K. Binder, J. Chem. Phys. **131**, 114907/1 (2009).

[32] T. Wuest, Y. W. Li, and D. P. Landau, J. Stat. Phys. **144**, 638 (2011), ISSN 0022-4715.

[33] A. D. Swetnam and M. P. Allen, J. Comput. Chem. **32**, 816 (2011), ISSN 1096-987X.

[34] M. Moeddel, W. Janke, and M. Bachmann, Macromolecules **44**, 9013 (2011), ISSN 0024-9297.

[35] M. Moeddel, W. Janke, and M. Bachmann, Comput. Phys. Commun. **182**, 1961 (2011), ISSN 0010-4655.

[36] N. Lesh, M. Mitzenmacher, and S. Whitesides, in *Proceedings of the 7th Annual International Conference on Research in Computational Molecular Biology*, edited by M. Vingron, S. Istrail, P. Pevzner, and M. Waterman (Association for Computing Machinery, New York, 2003), RECOMB, pp. 188–195, ISBN 1-58113-635-8.

[37] E. J. J. van Rensburg and S. G. Whittington, J. Phys. A Math. Gen. **24**, 5553 (1991).

[38] F. G. Wang and D. P. Landau, Phys. Rev. Lett. **86**, 2050 (2001).

[39] R. E. Belardinelli and V. D. Pereyra, Phys. Rev. E **75**, 046701/1 (2007).

[40] R. E. Belardinelli and V. D. Pereyra, J. Chem. Phys. **127**, 184105/1 (2007).

[41] C. Zhou and J. Su, Phys. Rev. E **78**, 046705/1 (2008).

[42] T. Vogel, M. Bachmann, and W. Janke, Phys. Rev. E **76**, 061803 (2007).

[43] T. Wüst and D. P. Landau, Phys. Rev. Lett. **102**, 178101/1 (2009).